LETTER

doi:10.1038/nature12832

Direct recording and molecular identification of the calcium channel of primary cilia

Paul G. DeCaen[1]*, Markus Delling[1]*, Thuy N. Vien[2] & David E. Clapham[1,3]

A primary cilium is a solitary, slender, non-motile protuberance of structured microtubules (9+0) enclosed by plasma membrane[1]. Housing components of the cell division apparatus between cell divisions, primary cilia also serve as specialized compartments for calcium signalling[2] and hedgehog signalling pathways[3]. Specialized sensory cilia such as retinal photoreceptors and olfactory cilia use diverse ion channels[4–7]. An ion current has been measured from primary cilia of kidney cells[8], but the responsible genes have not been identified. The polycystin proteins (PC and PKD), identified in linkage studies of polycystic kidney disease[9], are candidate channels divided into two structural classes: 11-transmembrane proteins (PKD1, PKD1L1 and PKD1L2) remarkable for a large extracellular amino terminus of putative cell adhesion domains and a G-protein-coupled receptor proteolytic site, and the 6-transmembrane channel proteins (PKD2, PKD2L1 and PKD2L2; TRPPs). Evidence indicates that the PKD1 proteins associate with the PKD2 proteins via coiled-coil domains[10–12]. Here we use a transgenic mouse in which only cilia express a fluorophore and use it to record directly from primary cilia, and demonstrate that PKD1L1 and PKD2L1 form ion channels at high densities in several cell types. In conjunction with an accompanying manuscript[2], we show that the PKD1L1–PKD2L1 heteromeric channel establishes the cilia as a unique calcium compartment within cells that modulates established hedgehog pathways.

Patch clamp of primary cilia is challenging due to their small dimensions (~0.2–0.5 μm in width, 1–12 μm in length), making them difficult to identify *in vivo*. Using a human retina pigmented epithelium cell line stably expressing the cilia-specific enhanced green fluorescent protein (EGFP)-tagged smoothened gene (hRPE SMO–EGFP), the cilia could be visualized under confocal fluorescence microscopy and recorded using the method we describe here: whole-cilia patch clamp (Fig. 1a, Extended Data Fig. 1a and Supplementary Video 1). After establishing >16 GΩ seals and rupturing the cilia membrane, we recorded a surprisingly large, outwardly rectifying, non-inactivating current (I_{cilia}). Notably, I_{cilia} was recorded from cilia attached or detached from the cell body (Fig. 1b, c and Supplementary Video 2). Current density measured in the detached cilia patch was 56-fold higher than that measured from the hRPE cell body (Methods). These measurements indicate that the primary cilium is partly insulated from the cell body by the structures at the cell–cilia junction (Extended Data Fig. 1a). The outwardly rectifying current was cation-non-selective (Fig. 1d) with relative permeabilities of $Ca^{2+} \approx Ba^{2+} > Na^{+} \approx K^{+} >$ NMDG (Extended Data Fig. 1b).

Consistent with the whole-cilia currents, single-channel amplitudes were outwardly rectifying (Fig. 1e) and mean open times substantially longer at more depolarized potentials. Extracellular uridine and adenosine phosphates (UDP, ADP, ATP) activated the ciliary current in perforated-cilia recordings, whereas the non-selective antagonists Gd^{3+} and ruthenium red blocked it (Extended Data Fig. 1c–e). Several cell-permeable calmodulin antagonists also activated the conductance. On the basis of the dimensions of the cilia, we estimate the average membrane surface area to be ~6.3 μm^2 (~0.063 pF). Assuming the entire outward rectifying current is carried by the 96-pS conductance, we estimate the primary cilia channel density to be 128 ± 13 channels μm^{-2}, similar to endogenous channel densities calculated from excitable tissue plasma membranes

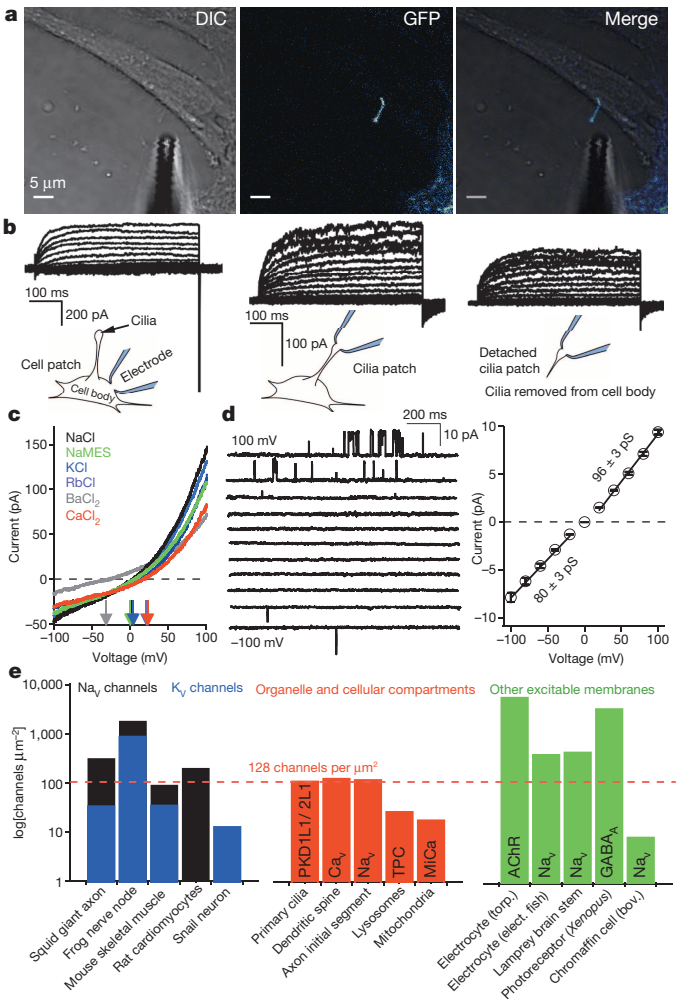

Figure 1 | A calcium-selective ion channel is richly expressed in primary cilia. **a**, Confocal image of an hRPE SMO–EGFP cell and patch-clamp electrode. **b**, Whole-cell leak-subtracted currents elicited by 1-s depolarizing pulses from −100 to 100 mV in +5-mV increments recorded from the cell body, primary cilia and an excised primary cilia (recorded from the same cilium). **c**, Whole-cell currents activated by ramp voltage protocols from −100 to +100 mV measured from the primary cilia where extracellular Na^{+}-based saline was replaced by the cation indicated. **d**, Single-channel currents activated by 1.5-s depolarizations to the indicated potentials (left) and average current amplitudes (right; ± s.e.m., $n = 8$ cilia). **e**, Estimated endogenous cilia ion channel densities compared to those from other biological preparations[17,27–30].

[1]Howard Hughes Medical Institute, Department of Cardiology, Children's Hospital Boston, 320 Longwood Avenue, Boston, Massachusetts 02115, USA. [2]Department of Neuroscience, Sackler School of Graduate Biomedical Sciences, Tufts University, Boston, Massachusetts 02111, USA. [3]Department of Neurobiology, Harvard Medical School, Boston, Massachusetts 02115, USA.
*These authors contributed equally to this work.

and larger than those found in intracellular compartments (Fig. 1f). Thus, the primary cilium is richly populated with Ca^{2+}-permeant, relatively non-selective cation channels that enable a much higher dynamic range of ciliary Ca^{2+} concentration compared to the cytoplasm.

We generated a transgenic mouse expressing the cilia-specific *Arl13b* gene carboxy-terminally tagged with EGFP (*Arl13b-EGFP*^{tg} mouse)[2] and isolated primary cells from mouse RPE (mRPE) and embryonic fibroblasts (MEFs). Primary cilia currents from these primary cells were outwardly rectifying with the same conductance and pharmacological properties as observed in the cilia from the human RPE cell line (Fig. 2 and Extended Data Fig. 2). In addition, I_{cilia} was observed in the cilia of a human kidney-derived inner medullary collecting duct cell line (IMCD stably expressing ARL–EGFP; Fig. 2c and Extended Data Fig. 2d). Ciliary single-channel conductances were identical in all four cell types (Fig. 2e), and were activated by extracellular ATP and blocked by Gd^{3+} in perforated patch recordings. ATP addition to the bath significantly increased the probability of channel opening (P_o) and mean open times (5–7-fold, Fig. 2f and Extended Data Fig. 2e). Because these were in the 'on-cilia' patch configuration (bath-applied ATP), we reasoned that ATP binds a G-protein-coupled purinergic receptor to initiate activation of the channels in the patch. Thus, I_{cilia} is a common feature of many cell types.

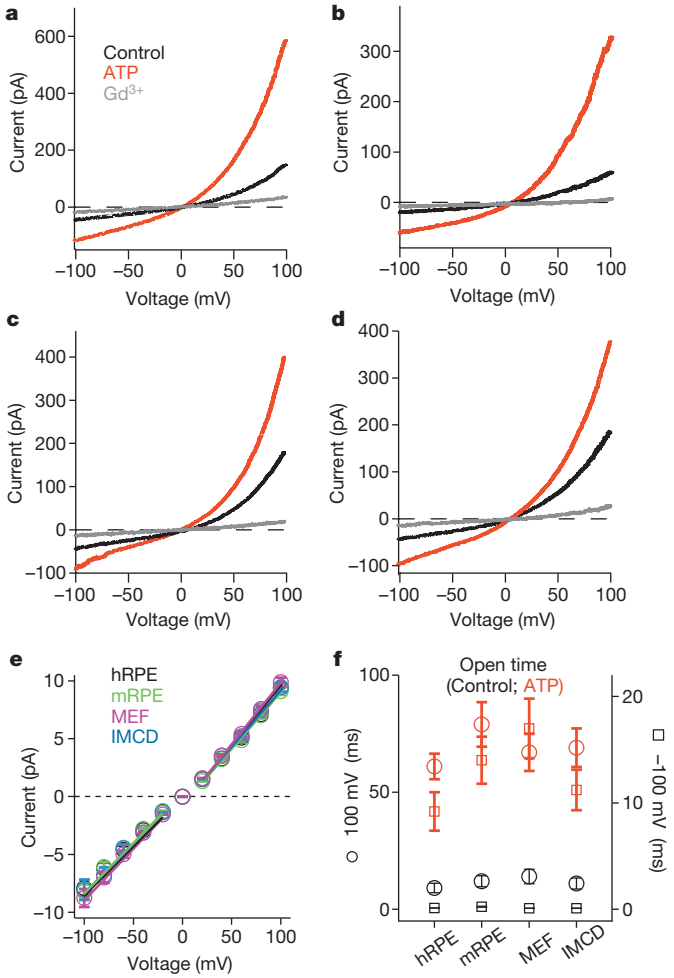

Figure 2 | Primary cilia currents measured from four different cell types. **a**–**d**, Averaged cilia current traces in control and bath-applied 100 μM ATP or 10 μM Gd^{3+} from: human RPE cell line stably expressing smoothened–EGFP (**a**); primary mRPE cells from the *Arl13b-EGFP*^{tg} mouse (**b**); kidney IMCD cell line stably expressing ARL–EGFP (**c**); and primary embryonic fibroblasts from the *Arl13B-EGFP*^{tg} mouse (**d**). **e**, Average single-channel current–voltage relation. The slope is used to estimate conductance (±s.e.m., $n = 4$–7 cilia). **f**, Average open times in the presence and absence of ATP at −100 and +100 mV potentials measured from the cilia of RPE SMO–EGFP cells (±s.e.m., $n = 6$ cilia).

Analysis of hRPE transcripts confirmed expression of several purported ciliary channels[13–16], including TMC7, TRPV4 and PKD1, PKD2, PKD1L1 and PKD2L1 (Extended Data Fig. 3a). Only short interfering (si)RNAs specific for PKD1L1 and PKD2L1 reduced both inward and outward currents (Extended Data Fig. 3c–d). These results indicate that I_{cilia} is conducted by either PKD1L1 or PKD2L1 independently, or together as a heteromeric ion channel. To verify I_{cilia} channel proteins, we patch clamped cilia of homozygous PKD2L1 knockout (*Pkd2l1*$^{-/-}$) crossed with *Arl13b-EGFP* mice. The much-reduced *Pkd2l1*$^{-/-}$ MEF ciliary current was linear and failed to activate when stimulated by calmidazolium (Fig. 3b, c). These data establish that PKD2L1 is a component of I_{cilia}.

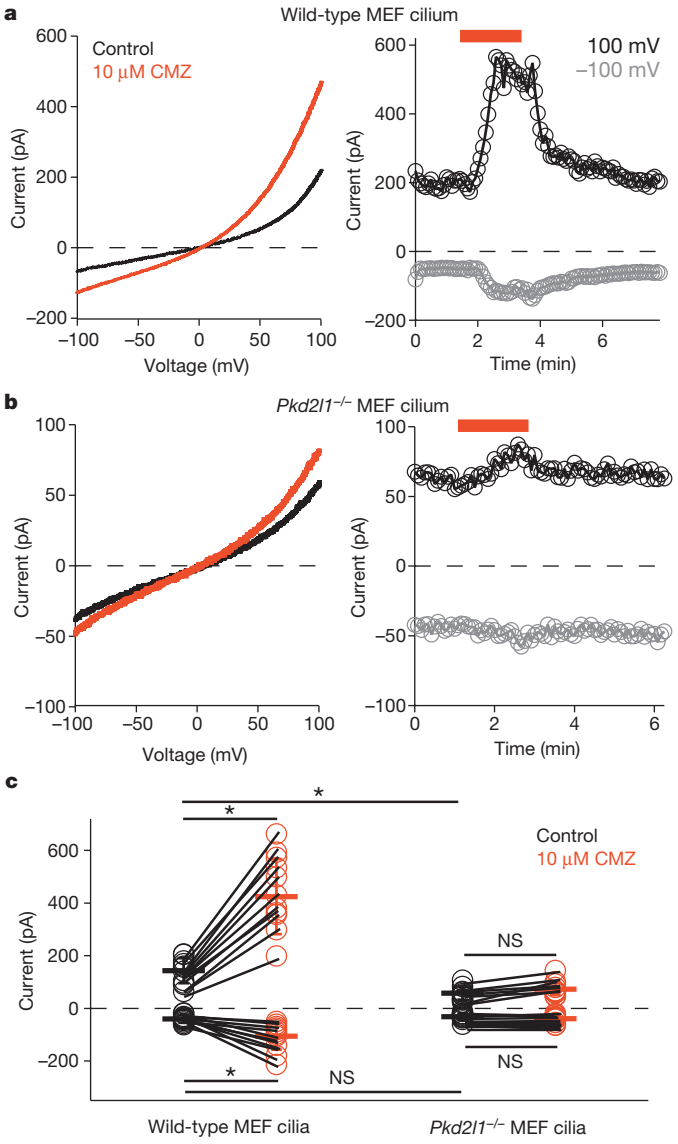

Figure 3 | MEF primary cilium currents compared from wild-type and *Pkd2l1* null animals. **a**, **b**, Left: cilium currents recorded from MEFs isolated from wild-type (**a**) and *Pkd2l1*$^{-/-}$ (**b**) mice. Currents were elicited by a series of ramps from −100 to +100 mV in control conditions (black traces) or in the presence of 10 μM calmidazolium (CMZ, red trace). Right: resulting current amplitudes (−100 mV, grey circles; +100 mV, black circles) plotted as a function of time. Red bar indicates application of extracellular 10 μM CMZ. **c**, Scatter and whisker (±s.d.) plots of current magnitudes at +100 mV and −100 mV from MEF cilia. Individual cilia are represented as connected circles in control (black) and after calmidazolium (red). Averages are indicated by the dark horizontal lines. Student's *t*-test results: $^*P < 0.05$; NS, $P > 0.05$; $n = 9$–11 cilia.

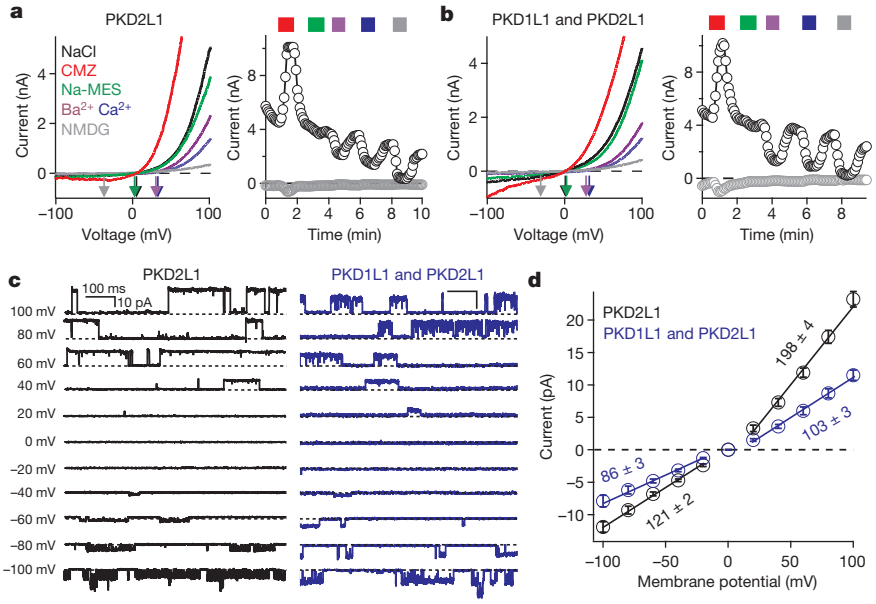

Figure 4 | Plasma membrane expressed PKD1L1–PKD2L1 channels match those of I_{cilia}. **a**, **b**, Whole-cell currents recorded from cells transfected with PKD2L1 alone (**a**) or PKD1L1 and PKD2L1 (**b**), where extracellular 1 μM calmidazolium (CMZ, red trace) was applied and Na^+-based saline was exchanged by the cations indicated. **c**, Single-channel currents measured from the cell membrane of cells transfected by PKD2L1 (black traces), or PKD1L1 and PKD2L1 (blue traces). **d**, Resulting average single-channel current amplitudes plotted against voltage measured from transfected cells (±s.e.m., $n = 4$–5 cells).

Immunoprecipitation of Flag- or haemagglutinin (HA)-tagged PKD1L1 and PKD2L1 demonstrated that PKD1L1 and PKD2L1 interact (Extended Data Fig. 4a). In whole-cell patch clamp of HEK293 cells transiently transfected with members of the PKD family, only PKD2L1 produced a measurable outward current in the plasma membrane (Extended Data Fig. 4b). Together, these data suggest that PKD2L1, but not PKD1L1, can form homomeric channels. On the basis of an alignment of the PKD2 family of proteins (Extended Data Fig. 4c), a cluster of conserved acidic residues in the putative selectivity filter[17] was mutated. Neutralizing two of three extracellular glutamates (Glu 523 and Glu 525, but not Glu 530) to serine or alanine abolished the current (Extended Data Fig. 4b). The homomeric PKD2L1 channel produced an outwardly rectifying, cationic whole-cell current with a large moderately Ca^{2+}-selective conductance (Fig. 4a and Extended Data Fig. 4d). Our results differ from the presumed PKD2L1 expressed in oocytes[18]: PKD2L1 currents in our HEK293T cells were outwardly rectifying and not activated by extracellular calcium. The unitary conductance (198 ± 3 pS) and rectification ratio of homomeric PKD2L1 is too large to underlie the primary ciliary conductance (compare Figs 1e and 4d). However, co-expression of PKD1L1 and PKD2L1 yielded a less rectifying whole-cell current with a single channel outward conductance of 103 ± 3 pS (Fig. 4b–d), consistent with that found in RPE primary cilia. In addition, heterologously expressed PKD2L1 and PKD1L1 channels were activated by calmodulin antagonists and blocked by Gd^{3+} and ruthenium red. Unlike the ciliary current, the heterologously expressed channels were not activated by extracellular uridine and purine analogues (UDP, ADP, ATP; data not shown), suggesting that the receptor/signal transduction pathway in cilia is absent in the whole-cell HEK293 conditions. These data establish that I_{cilia} is conducted by a heteromer of PKD1L1 and PKD2L1 subunits.

Primary cilia have been proposed to sense flow by mechanical activation of the putative PKD1–PKD2 channel[16,19]. Using pressure clamp[20], we observed no difference in single-channel activity at pressures of 0–60 mm Hg (8 kPa) for PKD1L1–PKD2L1 in mRPE primary cilia or in heterologous expression (Extended Data Fig. 5). Although channel activity measurably increased at high pressure (80–100 mm Hg; 11–13 kPa), the PKD1L1–PKD2L1 channel lacks the sensitivity found in designated mechanosensitive channels[21,22].

Many members of the TRP superfamily are highly temperature sensitive[7,23–25] and primary cilia are proposed to be temperature sensors via activation of a thermosensitive Ca^{2+} influx[26]. We tested the effect of increasing temperature (22–37 °C) on primary cilia and PKD1L1–PKD2L1-transfected cells and observed an increase in the Gd^{3+}-sensitive current (Extended Data Fig. 6a, b). When rapidly increasing the bath temperature (2.1 ± 0.2 °C s^{-1}), we observed biphasic current activation in the current from RPE primary cilia (from 24 to 32 °C, $Q_{10} = 6$) and heterologously expressed PKD1L1–PKD2L1 cilia (from 24 to 32 °C, $Q_{10} = 8$; Extended Data Fig. 6c). This sensitivity is moderate in comparison to highly temperature-sensitive channels, such as TRPV1–TRPV4 ($Q_{10} > 20$). In any case, temperature gradients are probably inconsequential over the length of cilia and cilia to cytoplasm.

The accompanying manuscript[2] demonstrated that cilia are a specialized calcium compartment containing the PKD1L1–PKD2L1 channel, which regulates ciliary SMO signalling and *Gli* transcription. Here we have demonstrated that PKD1L1 and PKD2L1 heteromultermerize to form a calcium-permeant ciliary channel which can be indirectly activated by purines. Future experiments will determine the purine receptor and downstream effectors activating I_{cilia}. Because the PKD1L1–PKD2L1 complex is calcium-permeant, but is also inactivated at high internal Ca^{2+} concentration, we propose that the channel regulates the high resting ciliary calcium level[2]. We propose that these signals modify regulation of smoothened target genes, in particular *Gli* transcription of genes regulating cell division and growth.

METHODS SUMMARY

Cilia were recorded via borosilicate glass electrodes polished to resistances of 13–19 MΩ. Holding potentials were −60 mV. Unless stated otherwise, pipette solutions contained (in mM): 100 CsMES, 35 NaCl, 10 HEPES, 5 Cs-BAPTA, 2 $MgCl_2$; 100 nM free [Ca^{2+}], pH 7.4. Standard bath solution (SBS) contained 150 NaCl, 10 HEPES, 1.8 $CaCl_2$, 1 $MgCl_2$, pH 7.4. For 'on cilia' recordings, the standard bath solution was: 150 KCl, 10 HEPES, 1.8 $CaCl_2$, 1 $MgCl_2$, pH 7.4 to clamp the resting membrane potential. For on-cilia recordings, the intracellular pipette solution was SBS. Perforated patches were obtained using 0.4 mg amphotericin B per 1 ml of standard intracellular saline. siRNA knockdown efficiency was monitored for every set of experiments with Silencer Negative Control 1 siRNA (Life Technologies) for controls. Sequences for gene-specific primers are listed in Extended Data Fig. 3a.

Additional experimental procedures are described in Methods.

Online Content Any additional Methods, Extended Data display items and Source Data are available in the online version of the paper; references unique to these sections appear only in the online paper.

Received 28 March; accepted 8 November 2013.

1. Bornens, M. The centrosome in cells and organisms. *Science* **335,** 422–426 (2012).
2. Delling, M., DeCaen, P. G., Doerner, J. F., Febvay, S. & Clapham, D. E. Primary cilia are specialized calcium signalling organelles. *Nature* http://dx.doi.org/10.1038/nature12833 (this issue).
3. Corbit, K. C. *et al.* Vertebrate Smoothened functions at the primary cilium. *Nature* **437,** 1018–1021 (2005).
4. Hardie, R. C. & Minke, B. The trp gene is essential for a light-activated Ca^{2+} channel in *Drosophila* photoreceptors. *Neuron* **8,** 643–651 (1992).
5. Shin, J. B. *et al. Xenopus* TRPN1 (NOMPC) localizes to microtubule-based cilia in epithelial cells, including inner-ear hair cells. *Proc. Natl Acad. Sci. USA* **102,** 12572–12577 (2005).
6. Stortkuhl, K. F., Hovemann, B. T. & Carlson, J. R. Olfactory adaptation depends on the Trp Ca^{2+} channel in *Drosophila*. *J. Neurosci.* **19,** 4839–4846 (1999).
7. Story, G. M. *et al.* ANKTM1, a TRP-like channel expressed in nociceptive neurons, is activated by cold temperatures. *Cell* **112,** 819–829 (2003).
8. Kleene, N. K. & Kleene, S. J. A method for measuring electrical signals in a primary cilium. *Cilia* **1,** 1–17 (2012).
9. Arnaout, M. A. Molecular genetics and pathogenesis of autosomal dominant polycystic kidney disease. *Annu. Rev. Med.* **52,** 93–123 (2001).
10. Celic, A., Petri, E. T., Demeler, B., Ehrlich, B. E. & Boggon, T. J. Domain mapping of the polycystin-2 C-terminal tail using *de novo* molecular modeling and biophysical analysis. *J. Biol. Chem.* **283,** 28305–28312 (2008).
11. Yu, Y. *et al.* Structural and molecular basis of the assembly of the TRPP2/PKD1 complex. *Proc. Natl Acad. Sci. USA* **106,** 11558–11563 (2009).
12. Zhu, J. *et al.* Structural model of the TRPP2/PKD1 C-terminal coiled-coil complex produced by a combined computational and experimental approach. *Proc. Natl Acad. Sci. USA* **108,** 10133–10138 (2011).
13. Gherman, A., Davis, E. E. & Katsanis, N. The ciliary proteome database: an integrated community resource for the genetic and functional dissection of cilia. *Nature Genet.* **38,** 961–962 (2006).
14. Andrade, Y. N. *et al.* TRPV4 channel is involved in the coupling of fluid viscosity changes to epithelial ciliary activity. *J. Cell Biol.* **168,** 869–874 (2005).
15. Raychowdhury, M. K. *et al.* Characterization of single channel currents from primary cilia of renal epithelial cells. *J. Biol. Chem.* **280,** 34718–34722 (2005).
16. Yoshiba, S. *et al.* Cilia at the node of mouse embryos sense fluid flow for left-right determination via Pkd2. *Science* **338,** 226–231 (2012).
17. Hille, B. *Ion Channels of Excitable Membranes* 3rd Edn (Sinauer Associates, 2001).
18. Chen, X. Z. *et al.* Polycystin-L is a calcium-regulated cation channel permeable to calcium ions. *Nature* **401,** 383–386 (1999).
19. Praetorius, H. A. & Spring, K. R. A physiological view of the primary cilium. *Annu. Rev. Physiol.* **67,** 515–529 (2005).
20. Besch, S. R., Suchyna, T. & Sachs, F. High-speed pressure clamp. *Pflugers Arch.* **445,** 161–166 (2002).
21. Coste, B. *et al.* Piezo proteins are pore-forming subunits of mechanically activated channels. *Nature* **483,** 176–181 (2012).
22. Sukharev, S. I., Blount, P., Martinac, B., Blattner, F. R. & Kung, C. A large-conductance mechanosensitive channel in *E. coli* encoded by mscL alone. *Nature* **368,** 265–268 (1994).
23. Xu, H. *et al.* TRPV3 is a calcium-permeable temperature-sensitive cation channel. *Nature* **418,** 181–186 (2002).
24. Benham, C. D., Gunthorpe, M. J. & Davis, J. B. TRPV channels as temperature sensors. *Cell Calcium* **33,** 479–487 (2003).
25. Voets, T. *et al.* The principle of temperature-dependent gating in cold- and heat-sensitive TRP channels. *Nature* **430,** 748–754 (2004).
26. Kottgen, M. *et al.* TRPP2 and TRPV4 form a polymodal sensory channel complex. *J. Cell Biol.* **182,** 437–447 (2008).
27. Cang, C. *et al.* mTOR regulates lysosomal ATP-sensitive two-pore Na^+ channels to adapt to metabolic state. *Cell* **152,** 778–790 (2013).
28. Fieni, F., Lee, S. B., Jan, Y. N. & Kirichok, Y. Activity of the mitochondrial calcium uniporter varies greatly between tissues. *Nature Commun.* **3,** 1317 (2012).
29. Shenkel, S. & Sigworth, F. J. Patch recordings from the electrocytes of Electrophorus electricus. Na currents and PNa/PK variability. *J. Gen. Physiol.* **97,** 1013–1041 (1991).
30. Brisson, A. & Unwin, P. N. Quaternary structure of the acetylcholine receptor. *Nature* **315,** 474–477 (1985).

Supplementary Information is available in the online version of the paper.

Acknowledgements P.G.D. was supported by NIH T32 HL007572. Animal work was, in part, supported by NIH P30 HD18655 to the IDDRC of Boston Children's Hospital. We thank B. Navarro, N. Blair, J. Doerner, S. Febvay, and the members of the Clapham laboratory for advice and assistance.

Author Contributions All authors designed or conducted experiments and wrote the manuscript.

Author Information Reprints and permissions information is available at www.nature.com/reprints. The authors declare no competing financial interests. Readers are welcome to comment on the online version of the paper. Correspondence and requests for materials should be addressed to D.E.C. (dclapham@enders.tch.harvard.edu).

METHODS

Electrophysiology. hRPE1 SMO–EGFP cells were serum starved 24–72 h before electrophysiological recording to slow cell growth and induce ciliogenesis. Primary cells cultured from the *Arl13b-EGFP*^{tg} mouse tissues (MEF and mRPE) were cultured for less than two passages before they were patch clamped. Data were collected using an Axopatch 200B patch clamp amplifier, Digidata 1440A, and pClamp 10 software. For temperature-controlled experiments, the perfusate was heated using a Warner TC-344B heater controller and in-line heater/cooler while bath temperature was monitored using a thermistor placed in close proximity to the recording electrode. For pressure-clamp experiments, membrane pressure was applied using a HSPC-1 high-speed pressure system (ALA Scientific) controlled by pClamp software. Whole-cell and excised inside-out patch currents were digitized at 25 kHz and low-pass filtered at 10 kHz. The permeability of monovalent cations relative to that of Na^+ was estimated from the shift in reversal potential on replacing external Na^+ bath solution (150 mM X, 10 mM HEPES, 0.5 mM $CaCl_2$, pH 7.4), where X was NaCl, NaMES, KCl, $BaCl_2$, $CaCl_2$, or NMDG. Permeability ratios were calculated as:

$$P_X = P_{Na}[Na^+]_{out}/[X]_{out} = \exp((F/RT)(V_{rev} - V_m))$$

where $[X]_{out}$ is defined as the extracellular concentration of the given ion, P is defined as the permeability of the ion indicated by the subscript, F is Faraday's constant, R is the gas constant, T is absolute temperature and V_{rev} is the reversal potential for the relevant ion.

Estimates of cilia channels per membrane surface area. The number of channels per cilia was calculated as $N = I/P_o(i)$, where $N =$ number of channels; I is the whole-cilium current at +100 mV; P_o is the open probability (calculated at +100 mV from ~1-s-long traces); and i is the single channel amplitude at +100 mV. Based on the slope of the single-channel records from RPE cilia, the channel conductance, $\gamma = 80 \pm 3$ pS inward and $\gamma = 96 \pm 3$ pS outward. RPE cilia channel mean open time at −100 mV and 100 mV were 0.22 ± 0.02 and 14 ± 3 ms, respectively. For simplification we represent the cilia as a cylinder and thus its surface area is given by $A = 2\pi r(r + h)$ where h is the height (5 μm on average) and radius (r) varies from 0.15 to 0.25 μm as measured in electron micrographs. Assuming $r = 0.2$ μm, then the surface area is ~6.3 μm^2 and capacitance (C_m, assuming 1 $\mu F\,cm^{-2}$) = 0.063 pF (for comparison, surface areas of typical cells are ~2,000 μm^2 with $C_m = 20$ pF). Current density measured in the detached cilia patch and the hRPE cell body was $1{,}730 \pm 98$ pA pF^{-1} and 31 ± 4 pA pF^{-1}, respectively. The equivalent circuit of the whole-cilia recording assumes that the resistance between cilia and cell is sufficiently high to neglect the contributions from the cell, as cilia ripped from the cell and sealed over show essentially the same result as cilia attached to the cell.

Plasmids and heterologous expression of PKD channels. HEK293T cells were transfected using Lipofectamine 2000 (Invitrogen) reagent. hPKD2, hPKD2L1 and hPKD2L2 cDNAs were obtained from Open Biosystems and a haemagglutinin (HA) tag was added to the amino terminus using PCR. The resulting cDNAs were subcloned into an IRES enhanced green fluorescence protein (EGFP)-containing vector. hPKD1L1 cDNA was synthesized (Bio Basic) with a Flag tag at the carboxy terminus. hPKD1L1, hPKD1 and hPKD1L2 were subcloned into an IRES red fluorescence protein (RFP)-containing vector. Transfected cells cultured at 37 °C and plated onto glass coverslips and were recorded 24–48 h later. For the co-transfected cells in Fig. 4, the cDNA was transfected at a 5:1 ratio for PKD1L1 and PKD2L1. Whole-cell patches for recordings from the cell body were obtained using electrodes of 1.5–2.5 MΩ and excised inside-out patches were obtained using pipettes of 5–7 MΩ resistances. Saline conditions are the same as those used for primary cilia.

Inhibition and detection of transcripts. SMO–EGFP expressing hRPE1 cells were transfected with 50 pM of siRNA and 5 μl RNAiMAX (Life Technologies) in a 3.5-cm dish. Cells were seeded at 230,000 cells per plate. 60 h after transfection, cells were serum-starved and cilia recordings performed 48 h after serum starvation. hRPE1 cells in a 3.5-cm dish were washed once with PBS and lysed in 1 ml Trizol for RNA extraction according to the manufacturer's instructions. RNA was reverse transcribed using the QuantiTect reverse transcription kit (Qiagen). Gene-specific primers were designed using Primerbank (http://pga.mgh.harvard.edu/primerbank/). Gene-specific products were amplified by PCR and gene expression was visualized by agarose gel electrophoresis.

Immunoprecipitation. HEK293T cells were transfected in a 10-cm dish with the indicated combinations of PKD1L1–Flag and PKD2L1–HA using Lipofectamine according to the manufacturer's instructions (Life Technologies). 24 h after transfection, cells were lysed in 2 ml RIPA buffer (20 mM Tris-HCl; pH 7.5, 150 mM NaCl, 1 mM EDTA, 1% NP-40 and 1% sodium deoxycholate with protease inhibitors added (Complete, Roche)). After centrifugation at 15,000*g* for 10 min at 40 °C, 1.5 ml of the supernatant was added to 30 μl anti-Flag M2 Agarose (Sigma-Aldrich) and incubated overnight at 40 °C. Agarose beads were spun down at 1,000*g* for 5 min and washed ×5 with RIPA buffer. The agarose beads were re-suspended in LDS samples buffer containing 2% β-mercaptoethanol, heated at 75 °C for 5 min, and proteins were separated on a 4–12% BisTris gel. After transfer to PVDF membrane, blots were probed with anti-Flag (Sigma Aldrich) or anti-HA (Roche) antibodies.

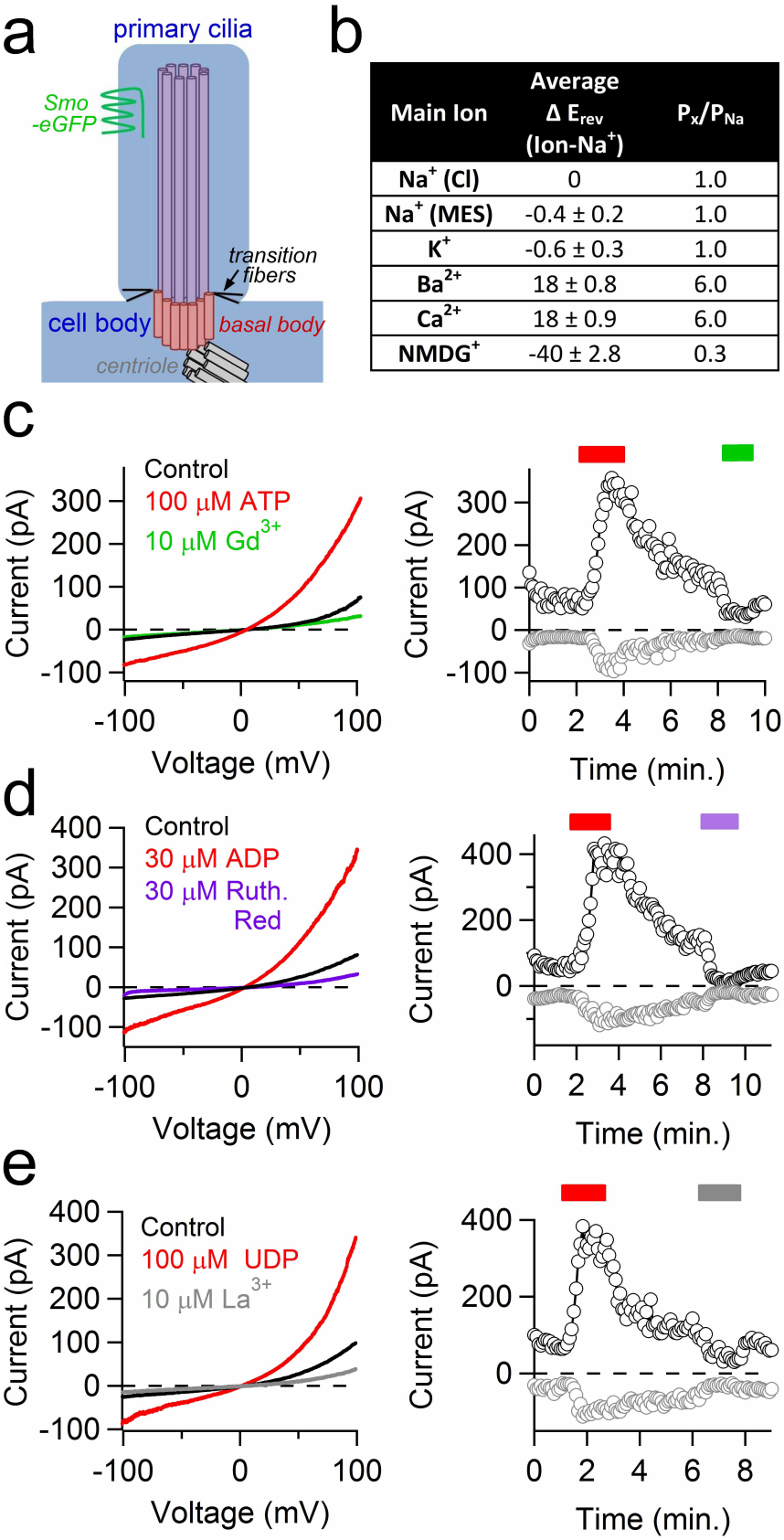

Main Ion	Average Δ E_{rev} (Ion-Na^+)	P_x/P_{Na}
Na^+ (Cl)	0	1.0
Na^+ (MES)	-0.4 ± 0.2	1.0
K^+	-0.6 ± 0.3	1.0
Ba^{2+}	18 ± 0.8	6.0
Ca^{2+}	18 ± 0.9	6.0
$NMDG^+$	-40 ± 2.8	0.3

Extended Data Figure 1 | Ion selectivity and pharmacology of ciliary hRPE current. **a**, Diagram of the primary cilia depicting the EGFP-labelled smoothened protein (green), transition fibres (black line), 9+0 axoneme (purple), basal body (pink) and centriole (grey). **b**, Table listing the average reversal potential change relative to the standard Na^+-based extracellular solution (average ΔE_{rev}) and the estimated relative permeability (P_x/P_{Na}; ±s.e.m., $n = 4$ cilia). **c**–**e**, Left: representative currents from control (black traces), activation by 100 μM ATP, 30 μM ADP, or 10 μM UDP (red traces) and block by 10 μM Gd^{3+}, 30 μM Ruthenium red and 10 μM La^{3+} (green, violet and grey traces, respectively). Right: corresponding time course of peak current recorded at −100 mV (grey circles) and +100 mV (black circles).

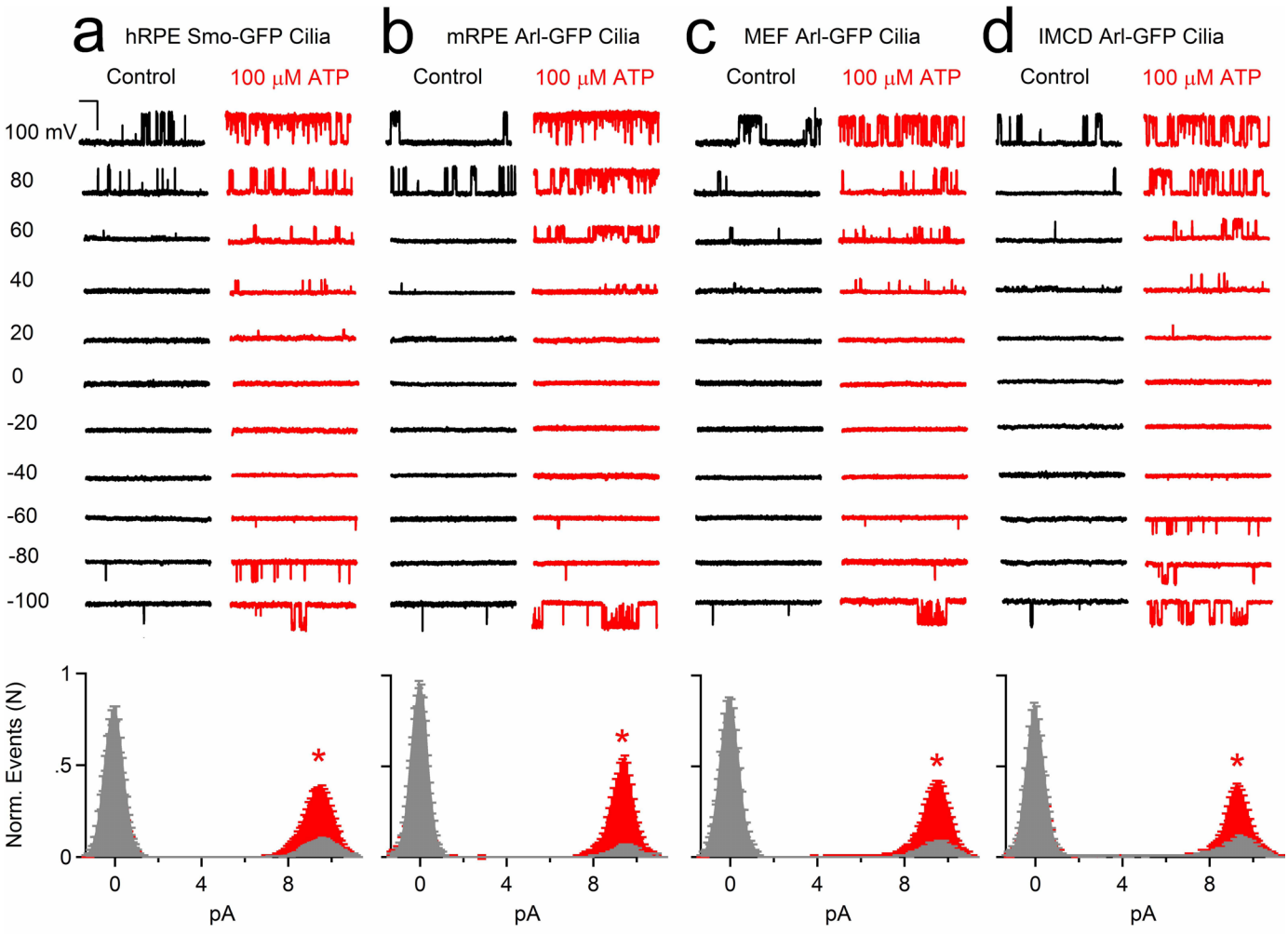

e

	100 mV		-100 mV	
Cell Type	*Control (ms)*	*ATP (ms)*	*Control (ms)*	*ATP (ms)*
hRPE (Smo-GFP)	14 ± 3	62 ± 5	0.22 ± 0.012	10 ± 2
mRPE (Arl-GFP)	12 ± 3	79 ± 6	0.43 ± 0.024	17 ± 3
MEF (Arl-GFP)	15 ± 3	67 ± 8	0.29 ± 0.024	19 ± 3
IMCD (Arl-GFP)	16 ± 2	72 ± 8	0.31 ± 0.036	12 ± 2

Extended Data Figure 2 | ATP indirectly activates the cilia conductance from four different cell types. **a–d**, Top: single-channel currents activated by 1.5-s depolarizations to the indicated potentials in control (black traces) and 100 μM extracellular ATP (red traces) recorded from primary cilia derived from human RPE SMO–GFP cell lines (**a**); mouse RPE ARL–GFP primary cells (**b**); mouse MEF ARL–GFP primary cells (**c**); and mouse kidney IMCD ARL–EGFP cells (**d**) (scale = 10 pA and 200 ms). Bottom: corresponding open probability histograms measured in control (grey) and in the presence of 100 μM ATP (red; ±s.e.m., $n = 4–6$ cilia, asterisks indicate $P < 0.005$). **e**, Average open dwell times measured from the cilia of these four cell types in control and ATP conditions.

a

Gene	up sequence 5'-3'	dn sequence 5'-3'
hMS4A5	CTGGGAGCAATAGCTGGAATC	CCAAAATTGAGAAAGGCAGAGA
hTMC7	TCCTGTTGGTGTTGTTGATCG	TGTGACACCATGGATGAAGGA
hTRPV4	ATTATGGCTTCTCGCATACCG	GCGGCTGGACTAGAAATGAGT
hPKD1-L1	TCCTTTGGTGGTGAGCTGTC	AGCATAGACCTCGACCCACA
hPKD2-L1	CCACCTTCACCAAGTTTGACA	GGGCTGCTCACAATAGATCG
hPKD1	CCGCTTCAAGTACGAGATCCT	CTCGGATCTTCCACACGCTAC
hPKD2	TGACTCTGAGGAGGATGACGA	TTGGCTCGCTCCATAATCTCT

b

siRNA against	Life technologies ID#	Knock down efficiency (SEM)
hPKD1	s10562	82 ± 4
hPKD1-L1	s46712	82 ± 2
hPKD1-L1	s46713	71 ± 4
hPKD2	104317	79 ± 3
hTRPV4	s34001	92 ± 2
hPKD2-L1	s17215	91 ± 3
hPKD2-L1	s17216	95 ± 3
hMS4A5	130501	78 ± 4
hTMC7	s33617	72 ± 5

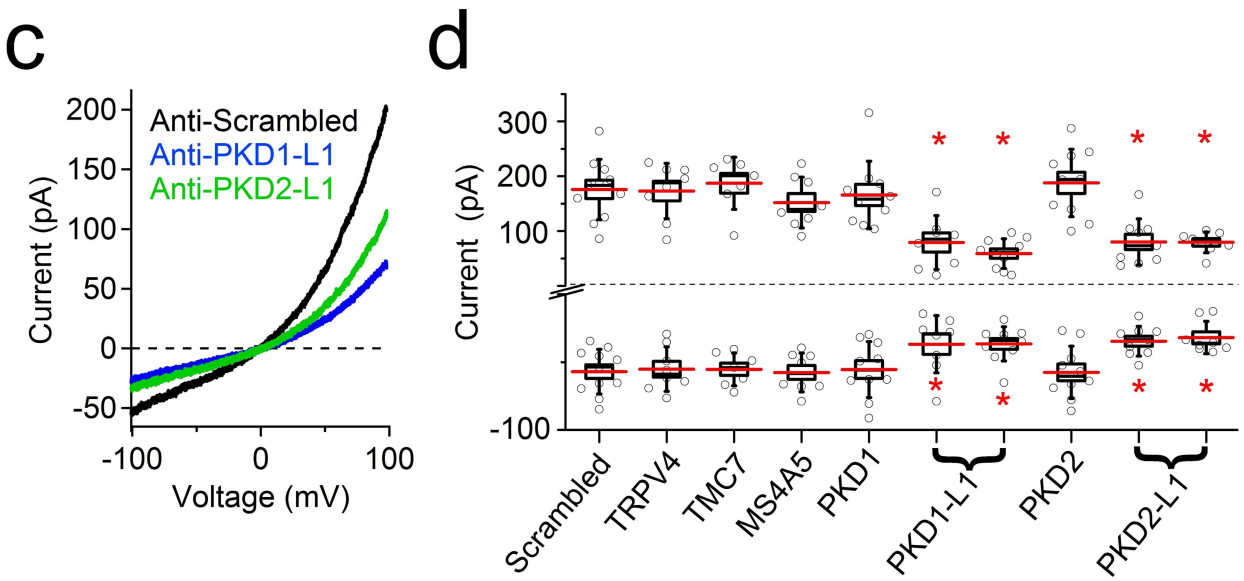

Extended Data Figure 3 | Anti-PKD1L1 and anti-PKD2L1 siRNA treatment attenuates the RPE ciliary current. **a**, Table of primers used to detect transcript levels present in human RPE cells. **b**, Table of siRNAs and their knockdown efficiencies used to identify channel candidates. **c**, Example ciliary current measured from cells treated with siRNAs specific for PKD1L1 or PKD2L1. **d**, Box (±s.e.m.) and whisker (±s.d.) plots of cilia total outward (+100 mV) and inward (−100 mV) current measured 72 h after double-siRNA treatment. PKDL mRNAs were targeted by two siRNAs specific for two different regions of the target transcript. Averages are indicated by the red lines. Student's *t*-test *P* values comparing treatment groups to scrambled siRNA; $^*P < 0.05$; $n = 8–12$ cilia.

a

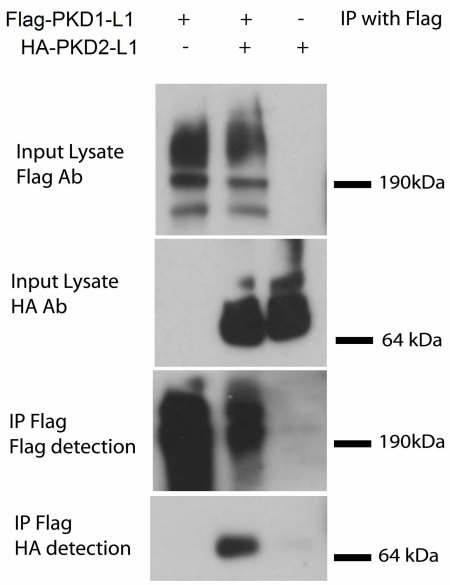

b

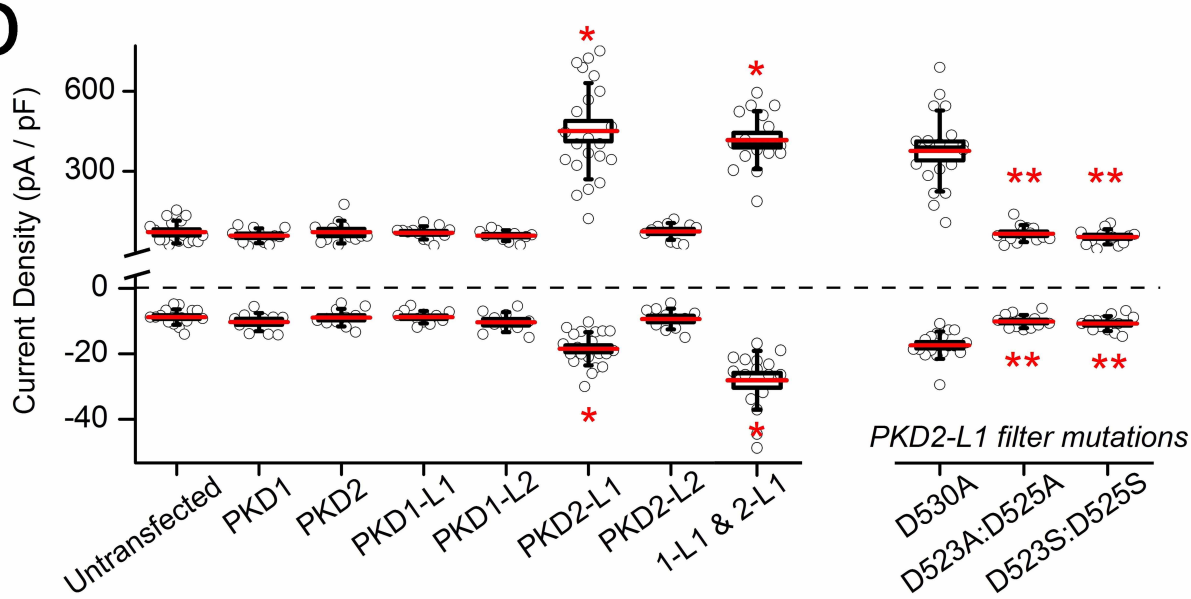

c

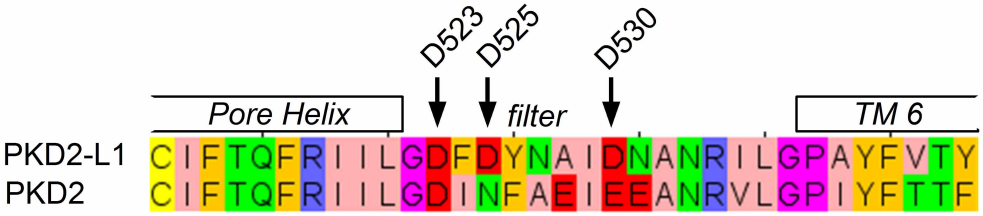

d

	PKD2-L1		PKD1-L1/2-L1	
Main Ion	Average Δ E_{rev} (Ion-Na^+)	P_x/P_{Na}	Average Δ E_{rev} (Ion-Na^+)	P_x/P_{Na}
Na^+ (Cl)	0	1.0	0	1.0
Na^+ (MES)	0.2 ± 0.1	1.0	0.3 ± 0.1	1.0
Ba^{2+}	19 ± 1.2	6.1	18 ± 1.4	6.1
Ca^{2+}	22 ± 0.8	6.3	20 ± 0.8	6.2
$NMDG^+$	-39 ± 3.1	0.3	-36 ± 3.0	0.2

Extended Data Figure 4 | Heterologous PKD1L1 and PKD2L1 form an ion channel. **a**, Immunoprecipitation of Flag– and HA–tagged PKD1L1 and PKD2L1 heterologously expressed in HEK293T cells. **b**, Box (±s.e.m.) and whisker (±s.d.) plots of the current densities measured from PKD1L1 and PKD2L1 family-transfected HEK cells at −100 mV (bottom) and +100 mV (top). Averages are indicated by the red lines. Statistical significances from Student's *t*-test comparing transfected to untransfected cells are indicated by asterisks ($P < 0.005$; $n = 10$–23 cells) and those comparing PKD2L1 to the pore mutants are indicated by double asterisks (*$P < 0.005$ compared to untransfected cells; **$P < 0.005$ compared to PKD1L1/PKD2L1 transfected cells; $n = 9$–11 cells). **c**, An alignment of the PKD2L1 and PKD2 (polycystin 2) pore helix and selectivity filter with glutamate residues D523, D525 and D530 indicated. **d**, Table listing the average reversal potential change relative to the standard Na^+-based extracellular solution (average ΔE_{rev}) and the estimated relative permeability (P_x/P_{Na}) for HEK cells transfected with PKD2L1 alone or with PKD2L1 and PKD1L1 (±s.e.m., $n = 4$–6 cells).

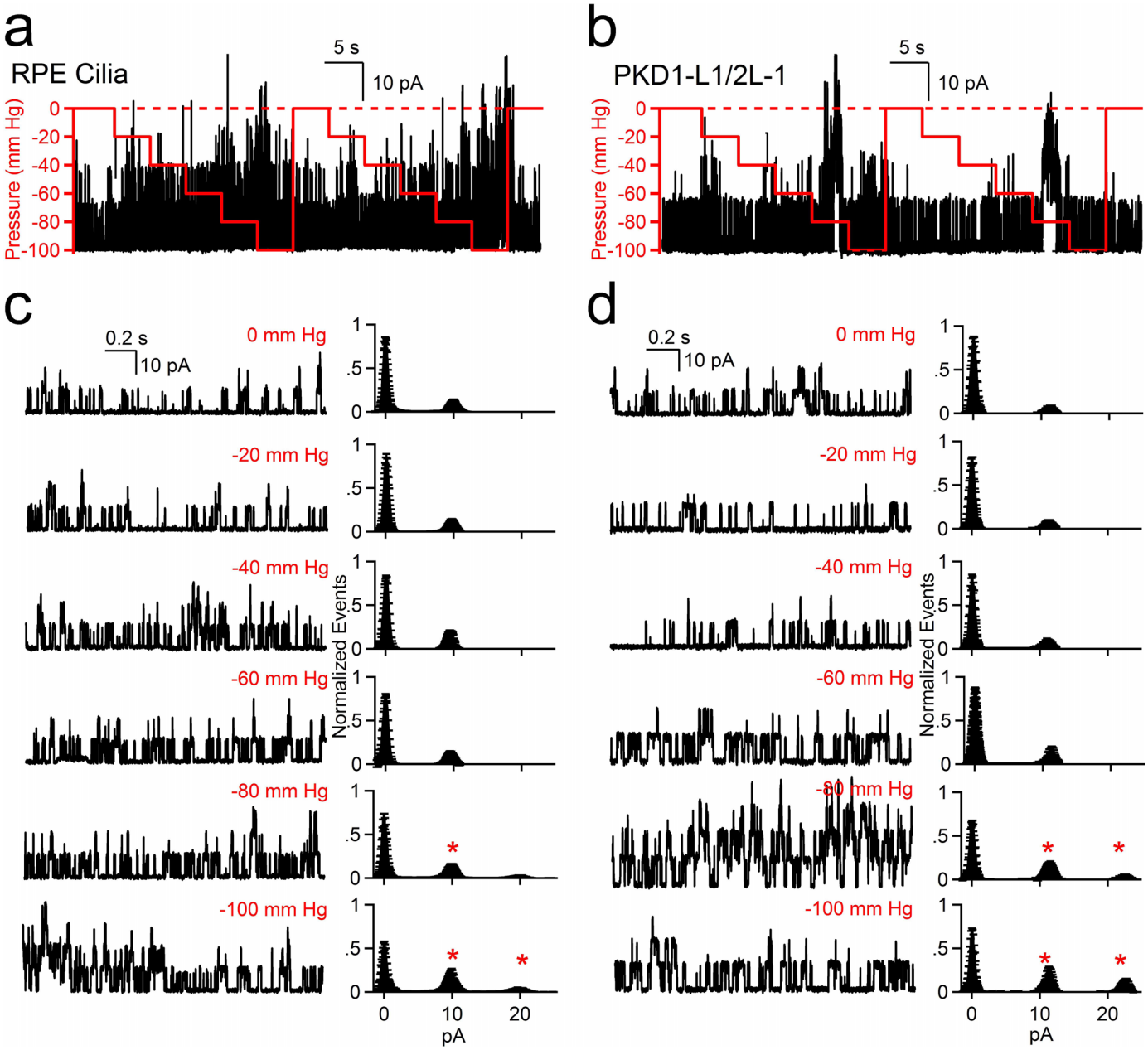

Extended Data Figure 5 | The PKD1L1–PKD2L1 channel is mechanosensitive only at high pressures. **a**, **b**, Results of pressure clamp (0–100 mm Hg, red line) on PKD1L1–PKD2L1 single channel events recorded from RPE primary cilia (**a**) and HEK293T cells (**b**) transfected with PKD1L1 and PKD2L1. **c**, **d**, Left: expanded times scales from **a** and **b**. Right: corresponding averaged normalized amplitude histograms are plotted for the indicated applied pipette (±s.e.m., $n = 5$ cilia and 6 cells). Cilia or cells were held at +100 mV and pressure changes were applied at 5-s intervals. Asterisks indicate a significant ($P > 0.05$) increase in channel opening events relative to the zero pressure condition.

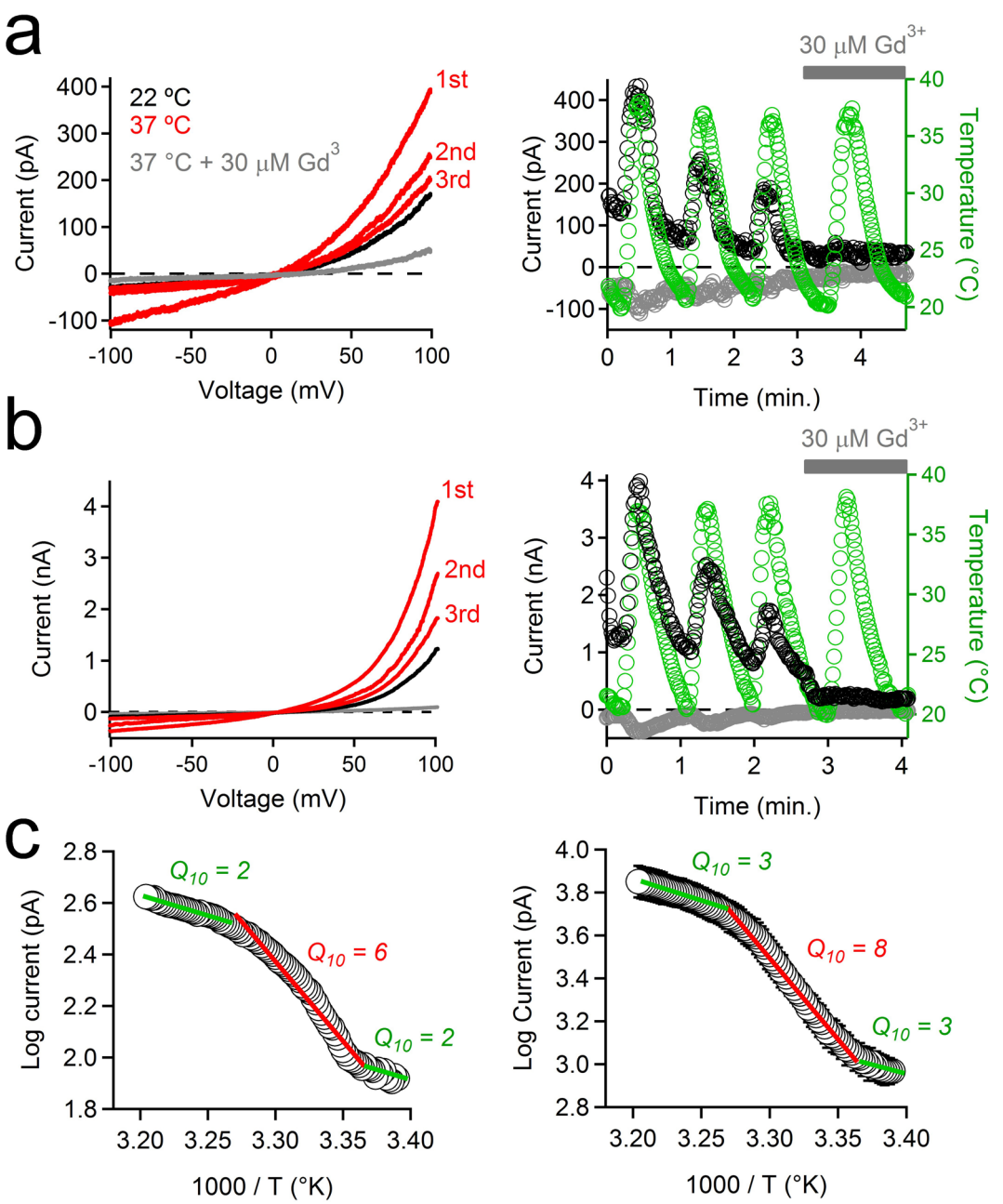

Extended Data Figure 6 | The PKD1L1–PKD2L1 channel is highly temperature sensitive. **a**, **b**, The effects of repeated temperature stimulations from 22 to 37 °C on the PKD1L1–PKD2L1 current recorded from RPE primary cilia (**a**) and HEK293T cells (**b**) (plasma membrane) transfected with PKD1L1 and PKD2L1. Left: currents elicited by a series of 1-Hz voltage ramps from −100 to +100 mV from 21 to 38 °C in control conditions (red traces) or in the presence of 30 μM Gd^{3+} (grey trace). Right: resulting current amplitudes (−100 mV, grey circles; +100 mV, black circles) and cilia temperature (green circles) are plotted as a function of time. Grey bar indicates the duration of extracellular 30 μM Gd^{3+} application. **c**, Arrhenius plots of the PKD1L1–PKD2L1 currents recorded from (left) RPE primary cilia and (right) when heterologously expressed in HEK293T cells. Q_{10} values were derived from three linear fits of the average normalized current magnitude from three phases of the thermal response (21–24 °C; 24–32 °C; 32–38 °C; ±s.e.m.; $n = 4$ cilia or 4 cells).

CORRIGENDUM

doi:10.1038/nature13631

Corrigendum: Direct recording and molecular identification of the calcium channel of primary cilia

Paul G. DeCaen, Markus Delling, Thuy N. Vien & David E. Clapham

Nature **504,** 315–318 (2013); doi:10.1038/nature12832

In this Letter, Fig. 1c and e contained errors, which are corrected in Fig. 1 of this Corrigendum. In the key of Fig. 1c, the extracellular conditions for the Ba^{2+} and NMDG currents were wrongly listed: the purple trace should be $BaCl_2$ (not RbCl) and the grey trace should be NMDG (not $BaCl_2$). This correction accurately reflects the selectivity of the channel as stated on page 315, which should have cited Fig.1c, rather than Fig. 1d, as follows: "The outwardly rectifying current was cation-non-selective (Fig. 1c) with relative permeabilities of $Ca^{2+} \approx Ba^{2+} > Na^{+} \approx K^{+} >$ NMDG". In Fig. 1e, the channel density for the primary cilia (red bar labelled 'PKD1L1/2L1') was wrong, owing to an incorrect estimation of open probability for the channel (0.015 instead of 0.067). This correction reduces the estimated channel density to a value (29 channels per μm^2) that is about 4.5 times smaller than the value we initially reported in Fig. 1 and on page 315 (128 channels per μm^2). This error does not alter the key findings of Fig. 1e (that the cilia are densely populated with PKD1L1/2L1 channels) or the main conclusions of the Letter.

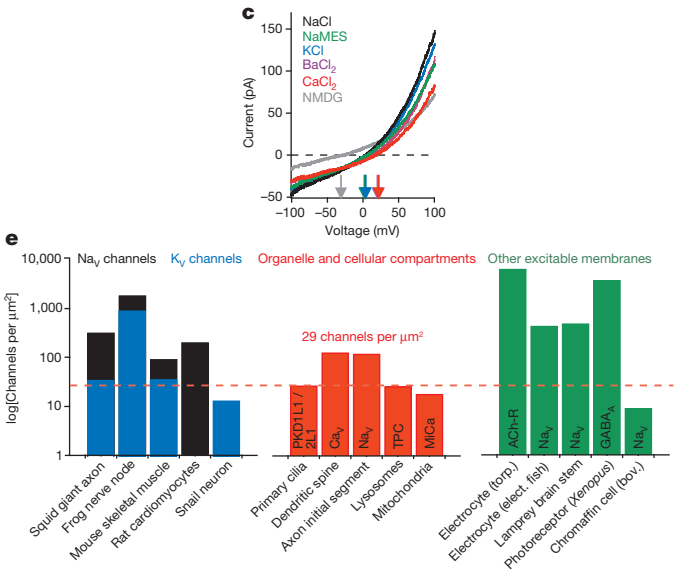

Figure 1 | This figure shows the corrected Fig. 1c and e of the original Letter.